# Recursion method in the k-space representation

S. M. Anlage
*Department of Applied Physics, California Institute of Technology, Pasadena, California 91125*

D. L. Smith
*Los Alamos National Laboratory, University of California, Los Alamos, New Mexico 87545*
(Received 14 April 1986)

We show that by using a unitary transformation to **k** space and the special-**k**-point method for evaluating Brillouin-zone sums, the recursion method can be very effectively applied to translationally invariant systems. We use this approach to perform recursion calculations for realistic tight-binding Hamiltonians which describe diamond- and zinc-blende-structure semiconductors. Projected densities of states for these Hamiltonians have band gaps and internal van Hove singularities. We calculate coefficients for 63 recursion levels exactly and for about 200 recursion levels to a good approximation. Comparisons are made for materials with different magnitude band gaps (diamond, Si, $\alpha$-Sn). Comparison is also made between materials with one (e.g., diamond) and two (e.g., GaAs) band gaps. The asymptotic behavior of the recursion coefficients is studied by Fourier analysis. Band gaps in the projected density of states dominate the asymptotic behavior. Perturbation analysis describes the asymptotic behavior rather well. Projected densities of states are calculated using a very simple termination scheme. These densities of states compare favorably with the results of Gilat-Raubenheimer integration.

## I. INTRODUCTION

The recursion method[1,2] is a general numerical technique for calculating projected densities of states of one-electron Hamiltonians expressed in a local orbital basis set. Because it is not based on symmetry properties, the recursion method is often used in the description of systems without translational symmetry such as disordered materials and defect structures. It can also be used to describe translationally invariant systems. In this case, the large number of matrix inversions necessary to calculate a projected density of states by Brillouin-zone integration techniques are avoided by using the recursion method. For materials which can be described with a small number of local orbitals in the basis set of each unit cell, the Brillouin-zone integration techniques are quite efficient. However, for more complex materials in which a large number of local orbitals in the basis set of each unit cell are required, Brillouin-zone integration can take a great deal of computer time. For these systems the recursion method can be advantageous.

In the recursion method,[1,2] an initial-state vector, on whose projection one wishes to calculate a density of states, is selected. Starting with this state, a new basis set is constructed by a three-term recursion relation. A series of recursion coefficients is also generated. The new basis set is of interest because the Hamiltonian is tridiagonal in this basis and its matrix elements are the recursion coefficients. From these matrix elements, the projected density of states is generated as a continued fraction. For an infinite system, the new basis set will, in general, have an infinite number of elements. In practice, of course, only a finite number of recursion levels can be calculated. Typically, the initially chosen state is localized in space and as the recursion proceeds, the generated state functions spread out in space. The number of recursion levels calculated is limited by the size of a cluster of atoms that can be treated. In a typical calculation with a realistic model Hamiltonian, a cluster of a few thousand atoms may be considered, which allows about 10—20 recursion levels to be exactly calculated. Various approaches have been suggested to construct the projected density of states from these finite sets of recursion coefficients.[3–6] In many cases, these approaches rely on a knowledge of the asymptotic behavior of the recursion coefficients. For calculations based on realistic model Hamiltonians, the asymptotic region is not usually reached.[6]

This paper has two purposes. First, we show that by using a unitary transformation to **k** space and the special-**k**-point method[7–9] for evaluating Brillouin-zone sums of smooth functions, the recursion method can be very effectively applied to translationally invariant systems. A large number of recursion coefficients can be calculated and the asymptotic region of behavior can be reached. Second, using this approach we numerically investigate the asymptotic behavior of the recursion coefficients for realistic model Hamiltonians. We explicitly consider the tight-binding Hamiltonians of the diamond- and zinc-blende-structure semiconductors proposed by Vogl *et al.*[10] For these Hamiltonians, we calculate coefficients for 63 recursion levels exactly. For a position space cluster, it would require more than 250 000 atoms for the calculation. Based on an extrapolation of calculated results using a smaller number of special **k** points in our **k**-space sums (the feature which limits the number of recursion coefficients that can be exactly calculated in this approach) we believe that the first $\sim 100$ recursion coefficients are numerically precise (better than 1%) and the next $\sim 100$ recursion coefficients are rather close. The asymptotic region of behavior sets in after about 30—40 recursion levels. The asymptotic region is investigated by

 

Fourier transformation. The projected densities of states are constructed from the recursion coefficients using a very simple interpolation procedure and the results are compared with those obtained using Gilat-Raubenheimer integration.[11]

The paper is organized in the following way: in Sec. II we describe our approach for evaluating the recursion coefficients of a translationally invariant material, in Sec. III we apply this approach to Hamiltonians describing diamond and zinc-blende semiconductors, and in Sec. IV we summarize our conclusions. Some details for constructing symmetric **k**-space functions are included in an appendix.

## II. THE RECURSION METHOD IN k SPACE

In the recursion method,[1,2] one selects a particular state function, $U_0$. The object of the calculation is to find the $U_0$ diagonal matrix element of the Green's function,

$$G_0(E)=\langle U_0 \mid (E-H)^{-1} \mid U_0 \rangle \ , \tag{1}$$

where $H$ is the Hamiltonian and $E$ is an energy. Such matrix elements can be related to quantities of physical interest. For example, the projected density of states is given by

$$\begin{aligned} n_0(E) &\equiv \sum_J |\langle U_0 \mid \psi_j \rangle|^2 \delta(E-\varepsilon_j) \\ &= -\frac{1}{\pi} \mathrm{Im} G_0(E+i\delta) \ , \end{aligned} \tag{2}$$

where $\psi_j$ is an eigenstate of $H$ with eigenvalue $\varepsilon_j$. Starting with $U_0$, normalized to unity, one generates a series of state functions $U_n$ and recursion coefficients $a_n$ and $b_n$ by

$$\tilde{U}_{n+1}=(H-a_n)U_n-b_nU_{n-1} \ , \tag{3a}$$

$$a_n=\langle U_n \mid H \mid U_n \rangle \ , \tag{3b}$$

$$b_n=(\langle \tilde{U}_n \mid \tilde{U}_n \rangle)^{1/2} \ , \tag{3c}$$

$$U_n=\frac{\tilde{U}_n}{b_n} \ , \tag{3d}$$

with the initial condition

$$U_{-1}=0 \ . \tag{3e}$$

Within the orthonormal basis $\{U_n\}$ the Hamiltonian is tridiagonal with matrix elements given by Eq. (3b) and

$$\langle U_n \mid H \mid U_{n+1} \rangle = \langle U_{n+1} \mid H \mid U_n \rangle = b_{n+1} \ . \tag{4}$$

The $U_0$ diagonal matrix element of the Green's function can be expressed as a continued fraction involving the recursion coefficients[1,2]

$$G_0(E)=\cfrac{1}{E-a_0-\cfrac{b_1^2}{E-a_1-\cfrac{b_2^2}{\ddots \\ \cfrac{}{E-a_{l-1}-b_l^2 t(E)}}}} \ . \tag{5}$$

For an infinite system, the basis set $\{U_n\}$ contains an infinite number of terms and the continued fraction of Eq. (5) has an infinite number of levels. In practice, of course, only a finite number of levels can be calculated. Thus the continued fraction must be terminated in some way. The function $t(E)$ in Eq. (5) represents this termination. Several approaches for selecting this terminating function have been proposed.[3-6]

As the recursion method is usually applied, the Hamiltonian and state functions, $U_n$, are described in terms of a localized basis set. We consider a crystal and take an orthonormal[12] local basis $\{\phi_{ib}(r)\}$ where $R_i$ labels lattice points and $b$ labels orbitals in the unit cell (both orbital site and type of orbital on a given site). The orbitals are taken to be real. The Hamiltonian and state functions $\{U_n\}$ in this basis are labeled by

$$\langle \phi_{ib} \mid H \mid \phi_{jb'} \rangle \equiv H_{ib;jb'}=H_{bb'}(\mathbf{R}_i-\mathbf{R}_j) \tag{6a}$$

and

$$\langle \phi_{ib} \mid U_n \rangle \equiv U_{nib} \ . \tag{6b}$$

In this basis, the recursion equations are

$$\begin{aligned} \tilde{U}_{n+1,i,b} &= \sum_{j,b'} (H_{ib;jb'}-a_n\delta_{ij}\delta_{bb'}) \\ &\quad \times U_{njb'}-b_nU_{n-1,i,b} \ , \end{aligned} \tag{7a}$$

$$a_n=\sum_{i,b,j,b'} U^*_{nib}H_{ib;jb'}U_{njb'} \ , \tag{7b}$$

$$b_n=\left[\sum_{i,b} \tilde{U}^*_{nib}\tilde{U}_{nib}\right]^{1/2} \ , \tag{7c}$$

$$U_{nib}=\frac{1}{b_n}\tilde{U}_{nib} \ . \tag{7d}$$

For crystalline materials, it is possible to construct orthonormal basis functions $\{\phi_{\mathbf{k}b}\}$ with Bloch symmetry

$$\phi_{\mathbf{k}b}=\frac{1}{\sqrt{N}}\sum_i e^{i\mathbf{k}\cdot(\mathbf{R}_i+\mathbf{V}_b)}\phi_{ib} \ , \tag{8}$$

where $\mathbf{V}_b$ is the displacement of the $b$th orbital site from the lattice point and $N$ is the number of unit cells in the crystal. In this basis, the Hamiltonian and state functions $\{U_n\}$ are given by

$$\begin{aligned} \langle \phi_{\mathbf{k}b} \mid H \mid \phi_{\mathbf{k}'b'} \rangle &= \delta_{\mathbf{k}\mathbf{k}'}H_{bb'}(\mathbf{k}) \\ &= \delta_{\mathbf{k}\mathbf{k}'}\left[e^{i\mathbf{k}\cdot(\mathbf{V}_{b'}-\mathbf{V}_b)}\sum_J e^{i\mathbf{k}\cdot\mathbf{R}_j}H_{bb'}(\mathbf{R}_j)\right] \end{aligned} \tag{9a}$$

and

$$\langle \phi_{\mathbf{k}b} \mid U_n \rangle \equiv U_{nb}(\mathbf{k})=\sum_J \frac{1}{\sqrt{N}}e^{-i\mathbf{k}\cdot(\mathbf{R}_j+\mathbf{V}_b)}U_{njb} \ . \tag{9b}$$

Note that the Hamiltonian is block diagonal. In this basis, the recursion equations are

$$\tilde{U}_{n+1b}(\mathbf{k})=\sum_{b'}[H_{bb'}(\mathbf{k})-a_n\delta_{bb'}]U_{nb'}(\mathbf{k}) - b_n U_{n-1b}(\mathbf{k}) , \tag{10a}$$

$$a_n=\sum_{\mathbf{k}}\sum_{b,b'} U^*_{nb}(\mathbf{k})H_{bb'}(\mathbf{k})U_{nb'}(\mathbf{k}) , \tag{10b}$$

$$b_n=\left[\sum_{k}\sum_{b}\tilde{U}^*_{nb}(\mathbf{k})\tilde{U}_{nb}(\mathbf{k})\right]^{1/2} , \tag{10c}$$

$$U_{nb}(\mathbf{k})=\frac{1}{b_n}\tilde{U}_{nb}(\mathbf{k}) . \tag{10d}$$

The recursion equations in the $R$-space basis [Eq. (7)] and in the $\mathbf{k}$-space basis [Eq. (10)] are exactly equivalent. They are related by a unitary transformation. However, the procedure for solving these two sets of equations and the necessary approximations will be quite different. In the $R$-space basis, a finite cluster of atoms must first be chosen so that the state vectors $U_n$ will be of finite length. For the usual case of interest, the initial-state vector, $U_0$, is localized in $R$ space on one, or at most a modest number, of orbitals $\phi_{ib}$. The Hamiltonian connects orbitals on nearby spatial sites. As the recursion number grows, the state vectors $U_n$ spread out in space. After some number of recursion levels, the state vector $U_n$ is no longer entirely contained in the cluster. The recursion calculation will no longer be exact for levels past this critical one. Various approximations have been suggested to continue the calculation past the critical recursion level.[1] In the $\mathbf{k}$-space basis, an infinite system can be considered. However, only a finite number of $\mathbf{k}$ points can be used. The Hamiltonian does not mix different $\mathbf{k}$ components. Thus, if the initial-state vector $U_0$ contained a finite (tractable) number of $\mathbf{k}$ components, the recursion calculation could be exactly performed. This case has been considered in Ref. 13. However, in the usual case of interest, $U_0$ is localized in $R$ space and thus includes $\mathbf{k}$ points throughout the Brillouin zone. Since only a finite number of $\mathbf{k}$ points can be included, the question becomes one of the accuracy of the Brillouin-zone sums in Eqs. (10b) and (10c). A major point of this paper is that by using the special-$\mathbf{k}$-point method to perform these sums, a large number of recursion levels can be exactly calculated and many more can be calculated to a good approximation.

To proceed with the analysis of the $\mathbf{k}$-space recursion equations, first notice that both of the $\mathbf{k}$-space sums can be written in the form

$$\sum_{\mathbf{k}} g(\mathbf{k})=\sum_{\mathbf{k}}\left[\sum_{j}\frac{e^{i\mathbf{k}\cdot\mathbf{R}_j}}{N}g(\mathbf{R}_j)\right] , \tag{11a}$$

where for the sum in Eq. (10b),

$$g(\mathbf{R}_j)=\sum_{i,i'}\sum_{b,b'} U^*_{n(\mathbf{R}_i+\mathbf{R}_j)b}H_{\mathbf{R}_i b;\mathbf{R}_{i'}b'}U_{n\mathbf{R}_{i'}b'} , \tag{11b}$$

and for the sum in Eq. (10c)

$$g(\mathbf{R}_j)=\sum_{i,b}\tilde{U}^*_{n(\mathbf{R}_i+\mathbf{R}_j)b}\tilde{U}_{n\mathbf{R}_i b} . \tag{11c}$$

(Of course only the $R_j=0$ term will contribute in the $\mathbf{k}$-space sum. But the individual $R_j$ contributions are not known, only the sum on $j$, $g(\mathbf{k})$, is known.) From Eqs. (11b) and (11c), we see that for both sums $g(R_j)$ has the form of a vector $[H_{R_i b;R_i b'}U_{nR_i b'}$ in Eq. (11b) and $\tilde{U}_{nR_i b}$ in Eq. (11c)], which is spatially centered with a second vector $[U_{n(R_i+R_j)b}]$, which is also spatially centered but has been displaced from the first vector by $R_j$. Therefore, as $|R_j|$ becomes large, $g(R_j)$ will become small. Indeed, at any given recursion level, $g(R_j)$ will vanish for $|R_j|$ greater than some value which depends on the recursion level. (We are assuming that the initial state is localized in space and that the Hamiltonian has a limited range.)

The special-$\mathbf{k}$-point method is effective at performing Brillouin zone sums for functions $g(\mathbf{k})$ with the properties described above.[8,9] In this approach, one first constructs a symmetric function:

$$f(\mathbf{k})=\frac{1}{n_T}\sum_{i} g(T_i\mathbf{k}) , \tag{12}$$

where $T_i$ are the symmetry operators of the lattice point group and $n_T$ are the number of such operators. Clearly the sums on $f(\mathbf{k})$ and $g(\mathbf{k})$ are equal and $f(\mathbf{k})$ has the symmetry of the Brillouin zone. The function $f(\mathbf{k})$ can be written as

$$f(\mathbf{k})=[g(0)+\sum_{m=1}^{\infty} f_m A_m(\mathbf{k})]/N , \tag{13a}$$

$$A_m(\mathbf{k})=\sum_{j\in m} e^{i\mathbf{k}\cdot\mathbf{R}_j} , \tag{13b}$$

$$f_m=\frac{1}{n_T}\sum_{i} g(T_i\mathbf{R}_m) , \tag{13c}$$

where $m$ labels shells of lattice points, the sum on $j$ in Eq. (13b) is over the lattice points on a given shell and $g(0)$ is $g(R_i)$ at $R_i=0$. To perform the $\mathbf{k}$-space sums one selects a set of $\mathbf{k}_i$'s and weights $\alpha_i$ such that

$$\sum_{i}\alpha_i A_m(\mathbf{k}_i)=0 , \tag{14}$$

for all $m\leq M$. Algorithms to select these special $\mathbf{k}$ points and weights are given in Refs. 8 and 9. Note that finding these points and weights is a purely geometrical problem. The $\mathbf{k}$-space sum is then approximated by

$$\sum_{\mathbf{k}} g(\mathbf{k})=g(0) \simeq\sum_{i}\alpha_i f(\mathbf{k}_i) =g(0)+\sum_{m>M} f_m\left[\sum_{i}\alpha_i A_m(\mathbf{k}_i)\right] . \tag{15}$$

If $f_m$ is zero for $m>M$, the integration scheme is exact. If $f_m$ is small for $m>M$, the integration scheme is valid. The accuracy of a recursion calculation in the $\mathbf{k}$-space basis is limited by the accuracy of the $\mathbf{k}$-space integration scheme. For initial states $U_0$ which are localized in space and Hamiltonians with a limited range, the coefficients $f_m$, which appear in the $k$-space integrals, vanish when $m$ exceeds a critical value, $L_n$, which depends on the level of recursion $n$. As the recursion level increases, $L_n$ increases. For $L_n<M$, the $n$th level of recursion is calcu-

lated exactly. The value of $M$ is determined by the number of special $\mathbf{k}$ points chosen. Thus, increasing the number of special $\mathbf{k}$ points increases the number of recursion levels that can be exactly calculated.

The symmetric functions $f(\mathbf{k})$ must be constructed from the functions $g(\mathbf{k})$ which are actually calculated. In principle, these functions can be constructed by simply performing the sums indicated in Eq. (12). However, it is almost always possible to use symmetry to simplify these sums. In the Appendix, we describe ways in which these sums can be simplified.

## III. CALCULATIONS FOR DIAMOND AND ZINC-BLENDE SEMICONDUCTORS

We consider the Hamiltonians proposed by Vogl *et al.*[10] to describe the diamond and zinc-blende crystal structure semiconductors. These Hamiltonians describe a nearest-neighbor tight-binding model with five orbitals, an $s$, three $p$, and an "excited $s$-state" $s^*$, on each of the two atoms in the unit cell. These Hamiltonians describe the valence bands and lowest conduction band reasonably well. Densities of states calculated using these Hamiltonians have band gaps and van Hove singularities. We calculate recursion coefficients starting with each of the orbitals of the basis set. For the diamond structure, the two atoms in the unit cell are the same and there is no difference between a calculation starting with an orbital centered on one of the atoms and a calculation starting with the corresponding orbital centered on the other atom. The $s$ and $s^*$ orbitals form one-dimensional representations of the $T_d$ point group.[14] Thus, as discussed in the Appendix, the symmetrizing sum in Eq. (12) is automatically accomplished [i.e., $f(\mathbf{k})=g(\mathbf{k})$, in this case]. The $p$ orbitals form a three-dimensional representation of the $T_d$ point group. Thus, as discussed in the Appendix, the symmetrizing sum in Eq. (12) is accomplished by starting each of the three $p$ orbitals in the recursion scheme and summing over the states generated in this way [i.e., $f(k)=\frac{1}{3}\sum_J g^J(k)$, where $J$ stands for $p_x$, $p_y$, and $p_z$. See Eq. (A17) of the Appendix]. Clearly, the results for the recursion coefficient must be the same for each of the three $p$ orbitals and a calculation for the $p$ orbitals takes about 3 times as long as for the $s$ orbitals.

We use the algorithm derived in Ref. 8 to generate the special $\mathbf{k}$ points and weights. For this algorithm, the first breakdown in the condition of Eq. (14) occurs for shells corresponding to the lattice points $a_0$ $(2N,0,0)$. The general failures are for shells corresponding to the lattice points $a_0$ $(2Nl_1,2Nl_2,2Nl_3)$, where $l_i$ are integers. Most of the calculations we report are for $N=16$, which requires 2992 special $\mathbf{k}$ points. For this case, the recursion calculation is exact; that is, the correction term in Eq. (15) is zero, through 63 levels of recursion. The first correction occurs at $n_c=64$. We also report a calculation with $N=8$, which requires 408 special $\mathbf{k}$ points and has the first correction at $n_c=32$ for comparison.

Although the $k$-space integration is not exact for $n \geq n_c$, we might expect that the results continue to be rather close for $n/n_c$ less than some number. By comparing results with $N=8$ with those for $N=16$ we conclude that the results continue to be numerically precise (in the sense that corrections to $a_n$ and $b_n$ are less than 1% of the amplitude of the variation of $a_n$ and $b_n$ with $n$ in the asymptotic region) for $n/n_c \lesssim 1.5$ and rather close (loosely defined) for $n/n_c \lesssim 3$.

In Fig. 1, we show calculated results for the recursion coefficients $a_n$ and $b_n$ as a function of $n$ starting the recursion with the $s$ orbital in Si. The coefficients are pointwise defined but a continuous curve is plotted for each of view. Results are shown for $n \lesssim 198$. As discussed above, the results are exact for $n \lesssim 63$, numerically precise for $64 \lesssim n \lesssim 100$, and "rather close" for $100 \lesssim n \lesssim 198$. As seen from the figure, both $a_n$ and $b_n$ have relatively large amplitude structure at small $n$ which decays to an approximately constant amplitude oscillation in the asymptotic region. The asymptotic region sets in at $n \gtrsim 30$.

As has been discussed previously,[15–17] internal van Hove singularities in the projected density of states result in damped oscillations in the recursion coefficients and band gaps result in undamped oscillations. A perturbation analysis[16,17] suggests that in the asymptotic region the recursion coefficients should take the form

$$a_n = a + \sum_i \delta a_i \cos(\theta_i n - \omega_i) \tag{16a}$$

and

$$b_n = b + \sum_i \delta b_i \cos(\phi_i n - \gamma_i)\ , \tag{16b}$$

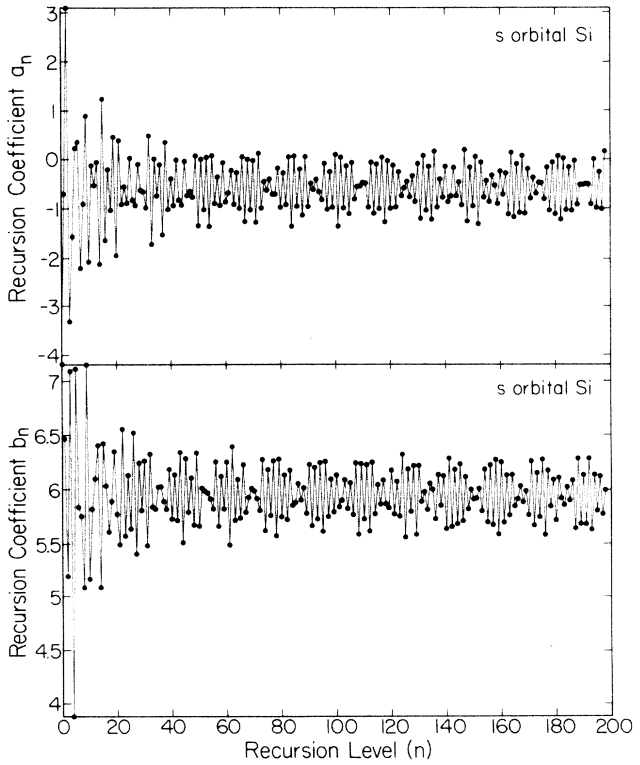


FIG. 1. The calculated recursion coefficients $a_n$ (upper panel) and $b_n$ (lower panel) as a function of recursion level $n$ starting the recursion with the $s$ orbital of Si.

where the sum is over the gaps in the projected density of states, $\delta a_i$ and $\delta b_i$ are related to the magnitude of the gaps, $\theta_i$ and $\phi_i$ are related to the energy position of the gaps, $a$ is the energy center of the projected density of states, and $b$ is one-fourth of the bandwidth. The frequencies ($\theta_i$ and $\phi_i$), phase angles ($\omega_i$ and $\gamma_i$), and amplitudes ($\delta a_i$ and $\delta b_i$) are related to each other by the perturbation analysis, but for comparison we will take them as independent.

For the model used here, Si has two band gaps: the main gap of 1.16 eV centered at 0.58 eV (the valence-band maximum defines the energy zero for these Hamiltonians) and a small gap (an artifact of the model Hamiltonian) of 0.17 eV centered at 6.58 eV. The main gap dominates the asymptotic region. There is a single dominant undamped sinusoidal oscillation. The apparent modulation is due to the fact that the recursion coefficients are only pointwise defined and the frequencies $\phi$ and $\theta$ are close to $\pi$.

In Fig. 2, we show calculated results for the recursion coefficients, $a_n$ and $b_n$, as a function of $n$ starting the recursion with the As $s$ orbital of GaAs. For the model used here, GaAs has two band gaps: the valence- to conduction-band gap of 1.55 eV centered at 0.77 eV and a valence-band gap of 2.47 eV centered at $-8.73$ eV. The valence-band gap occurs in the zinc-blende-structure materials, like GaAs, but not in the diamond-structure semiconductors. The two gaps of comparable size cause the asymptotic behavior for GaAs to be quite diffeent than that of Si which has a single dominant gap. For GaAs, there are two principal undamped frequency components corresponding to the two principal gaps.

In Figs. 3 and 4, we show calculated results for the recursion coefficients, $a_n$ and $b_n$, as a function of $n$ starting the recursion with the $s$ orbitals in diamond and $\alpha$-Sn, respectively. Diamond has a single valence- to conduction-band gap of 5.33 eV centered at 2.66 eV. $\alpha$-Sn is a semimetal and does not have a band gap.[18] It does, however, have two cusps (zeros) in the density of states at 0.0 and $-8.46$ eV. The asymptotic region of the recursion coefficients for diamond is similar to that of Si except that the amplitude of the undamped oscillations is much larger in diamond than in Si. The increased amplitude in diamond reflects its much larger band gap. In $\alpha$-Sn, which does not have a band gap, oscillations in the recursion coefficients are damped. The damping is quite slow, however, owing to the cusps in the density of states.

The calculations shown in Figs. 1–4 used 2992 special **k** points and the results are exact through $n=63$. The recursion coefficients shown in these figures appear to have reached asymptotic behavior for $n \gtrsim 30$. From simply viewing these figures, there is no obvious breakdown in the calculation for $n \lesssim 198$. In order to estimate the accuracy of the results for $n \geq n_c = 64$, we compare the above results with those of calculations using 408 special **k** points which have $n_c = 32$. Here, we specifically describe the case of $s$ orbitals in Si, but the behavior for the other

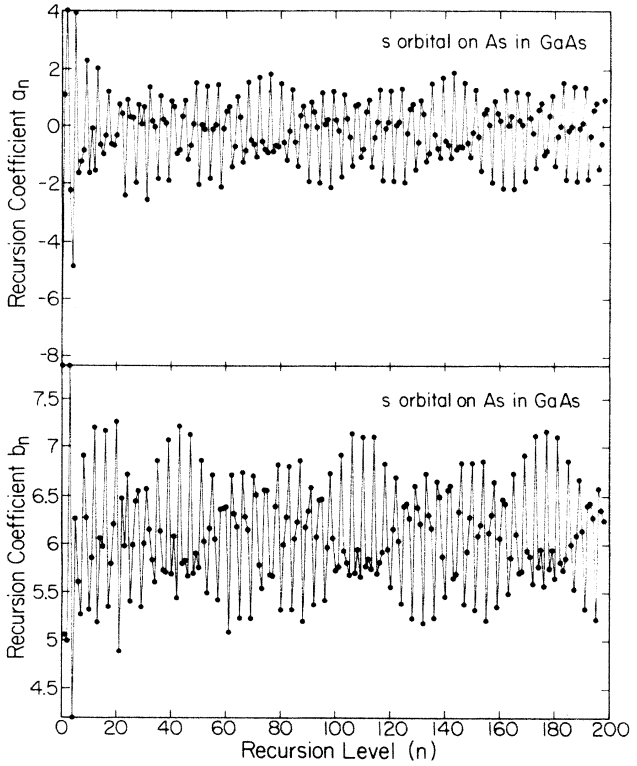


FIG. 2. The calculated recursion coefficients $a_n$ (upper panel) and $b_n$ (lower panel) as a function of recursion level $n$ starting the recursion with the As $s$ orbital of GaAs.

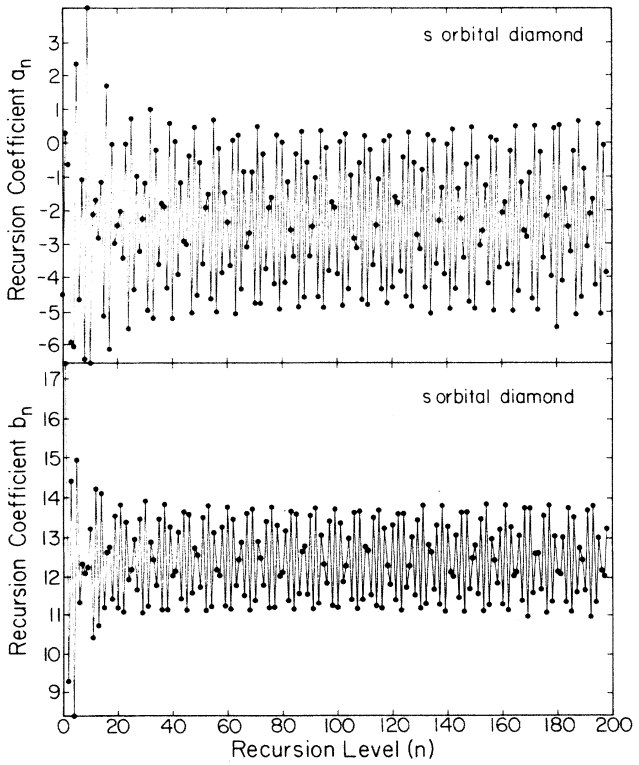


FIG. 3. The calculated recursion coefficients $a_n$ (upper panel) and $b_n$ (lower panel) as a function of recursion level $n$ starting the recursion with the $s$ orbital of diamond.

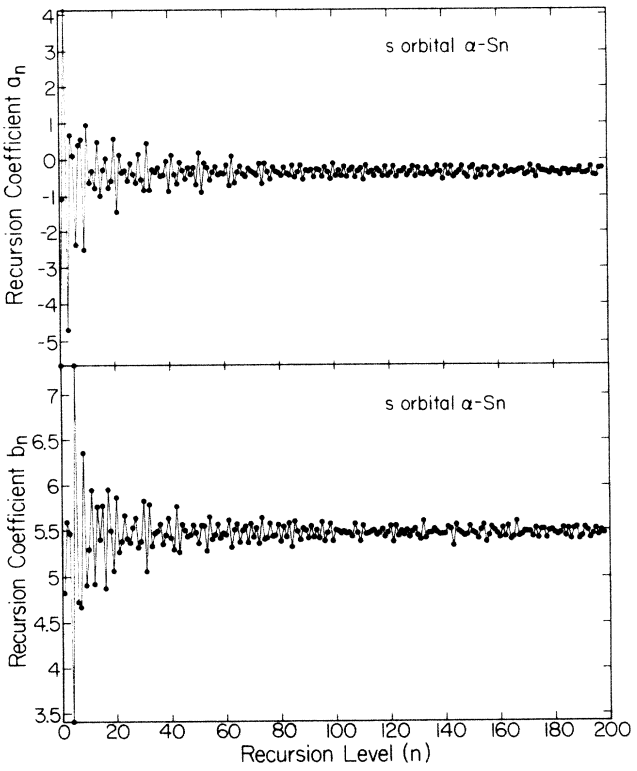


FIG. 4. The calculated recursion coefficients $a_n$ (upper panel) and $b_n$ (lower panel) as a function of recursion level $n$ starting the recursion with the $s$ orbital of $\alpha$-Sn.

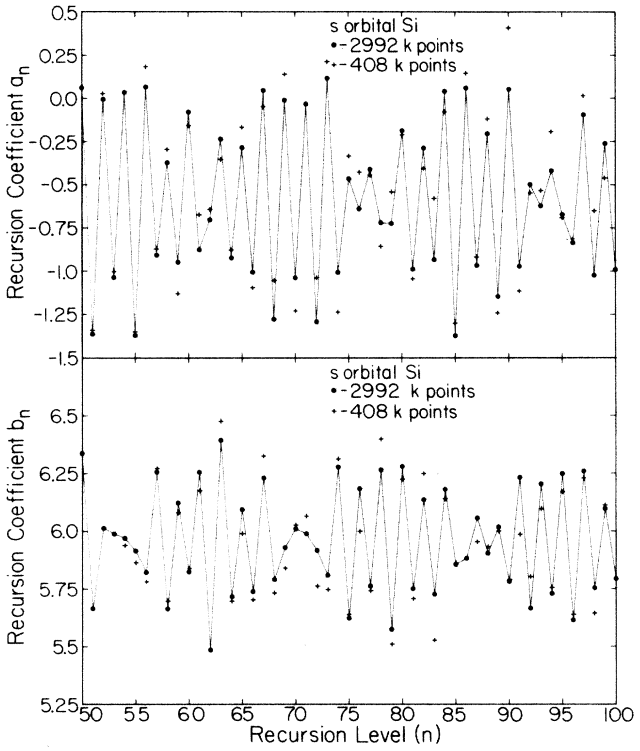


FIG. 5. Comparison of the recursion coefficients $a_n$ (upper panel) and $b_n$ (lower panel) for $n$ between 50 and 100, calculated using 2992 special **k** points (solid circles) with those calculated using 408 special **k** points (crosses).

systems is essentially the same. For $n < 32$, both calculations are exact and the results are the same. Writing out the calculated results to six significant figures, the first observed difference between the two calculations occurred at $n=40$. At $n=50$, the difference between the calculations first exceed 1% of the asymptotic oscillation amplitude. In Fig. 5, we compare the results of the two calculations for $50 \leq n \leq 100$. For these values of $n$, the results are rather close. The correspondence between the two results is lost for larger values of $n$ and the calculation using 408 special **k** points loses its periodic behavior. On the basis of this comparison, and very similar results for the other cases, we suggest that the results are numerically precise for $n/n_c \lesssim 1.5$ and rather close for $n/n_c \lesssim 3$.

Both the oscillatory behavior of the recursion coefficients in the asymptotic region that is apparent in Figs. 1–3 and the perturbation analysis,[16,17] which leads to Eqs. (16), suggests the utility of a Fourier analysis of the recursion coefficients. We perform a discrete Fourier transform of the region $30 \leq n \leq 198$. For this purpose, we define

$$a_n = A_0 + \sum_{j=1}^{84} A_j \cos\left[\left[\frac{2\pi}{169} j\right](n-30)\right] + \sum_{j=1}^{84} B_j \sin\left[\left[\frac{2\pi}{169} j\right](n-30)\right] . \quad (17)$$

An analogous transform is performed on the $b_n$ coefficients. Equation (17) is inverted to find $A_0$, $A_j$, and $B_j$. In Fig. 6, we show the coefficients $A_j$ and $B_j$ which result from the transform of the $a_n$ recursion coefficients for the $s$ orbital in Si.[19] There is a dominant feature in both $A_j$ and $B_j$ at $j=79$. Smaller features appear at $j=50$ and 47. Similar features occur at these channel numbers in the transform of $b_n$. The feature at $j=79$ corresponds to the main band gap in Si, the feature at $j=50$ corresponds to the small gap in the conduction band in this model, and the feature at $j=47$ corresponds to the cusp that occurs in in the Si valence band.

In Fig. 7, we show the Fourier transform coefficients $A_j$ and $B_j$ for the $a_n$ recursion coefficients for the As $s$ orbital in GaAs.[19] There are two dominate features at $j=81$ and 43. Similar strong features occur at these channel numbers in the transform of $b_n$. The feature at $j=81$ corresponds to the main valence to conduction-band gaps of GaAs and the feature at $j=43$ corresponds to the large valence to valence-band gap of GaAs.

Comparing Eq. (17) with the perturbation Eq. (16), one can extract the perturbation parameters characterizing the band gaps. The perturbation analysis[16,17] predicts relations between the perturbation parameters and the band gaps:

$$\phi_i = \theta_i , \quad (18a)$$

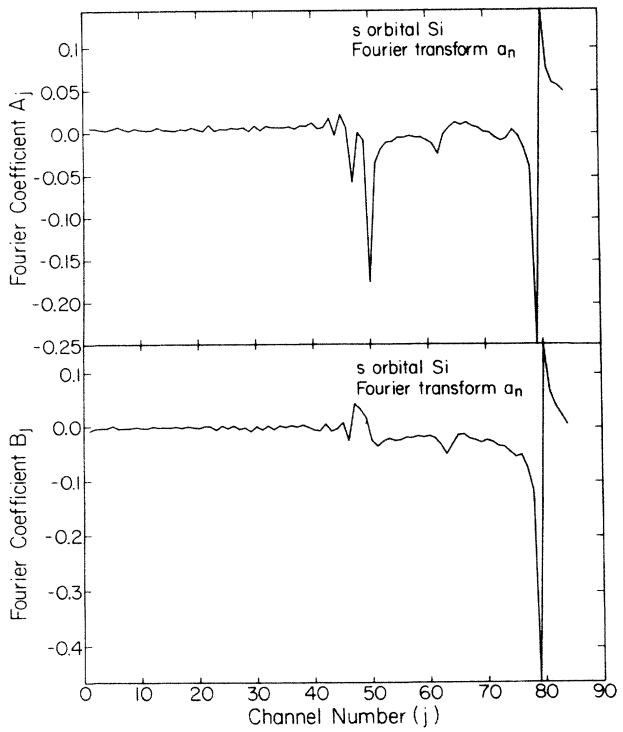


FIG. 6. The Fourier coefficients $A_j$ (upper panel) and $B_j$ (lower panel) which result from the transformation of the $a_n$ recursion coefficients starting the recursion with the $s$ orbital of Si.

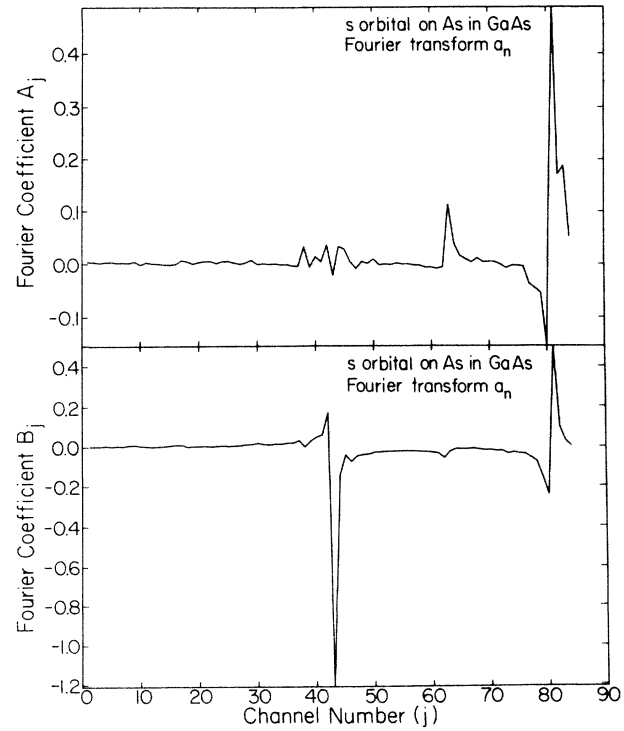


FIG. 7. The Fourier coefficients $A_j$ (upper panel) and $B_j$ (lower panel) which results from the transformation of the $a_n$ recursion coefficient starting the recursion with the As $s$ orbital of GaAs.

$$\Delta E_i = 2\,\delta a_i = 4\,\delta b_i \ , \tag{18b}$$

$$g_i = a \pm 2b\cos(\phi_i/2) \ , \tag{18c}$$

$$\omega_i = \gamma_i + \phi_j/2 \ \ (-\pi) \ , \tag{18d}$$

$$B = 4b \ , \tag{18e}$$

$$C = a \ , \tag{18f}$$

where $\Delta E_i$ is the size of the band gap, $g_i$ is the midpoint energy of the band gap, the $(-\pi)$ in Eq. (18d) and minus sign in Eq. (18c) are included for gaps in the lower-energy half of the spectrum and not in the upper-energy half, $B$ is the width of the energy spectrum, and $C$ is the energy midpoint of the spectrum. In Tables I and II, we compare these relations for the two gaps in Si and GaAs, respectively. The perturbation analysis parameters in these tables are from the Fourier analysis shown in Figs. 6 and 7 and analogous results for the $b_n$ coefficients. The band-gap parameters in the tables are from diagonalizing the Hamiltonian.

Major features in the Fourier analysis of the $a_n$ and $b_n$ coefficients occur in the same channel. Thus Eq. (18a) is satisfied to the accuracy of the analysis. From the comparison in the tables, one sees that the perturbation theory predictions are reasonably well satisfied in these cases. The largest discrepancies occur for the size of the small conduction to conduction-band gap in Si. The $s$ orbitals of Si are very weakly weighted in this energy region, as will be seen when this projected density of states is shown. In particular the edges of the band gap in the $s$ orbital projected density of states are very soft. Thus it may not be surprising that the perturbation analysis gives somewhat too large of a value for this gap.

The band gaps and band edges for the various projected densities of states in a given material are the same. One would thus expect that the Fourier analysis of the asymptotic region for different orbitals in a given material would yield similar results. This is indeed the case. For example, $s$, $s^*$, and $p$-orbital recursion coefficients in Si all show a dominant feature at $j=79$ and secondary features at $j=50$ and (valence-band cusp) in their Fourier

TABLE I. Comparison of band-gap and perturbation parameters, $s$ orbital in Si.

| Channel | $j=79$ | $j=50$ |
|---|---|---|
| $2\,\delta a_i$ (eV) | 1.06 | 0.36 |
| $4\,\delta b_i$ (eV) | 1.04 | 0.33 |
| $\Delta E_i$ (eV) | 1.16 | 0.17 |
| $a \pm 2b\cos(\theta_i/2)$ (eV) | 0.64 | 6.55 |
| $g_i$ (eV) | 0.58 | 6.58 |
| $\omega_i/\pi$ | 0.70 | 0.71 |
| $(\gamma_i+\theta_i/2)/\pi$ | 0.72 | 0.65 |
| $4b$ (eV) | 23.81 | |
| $B$ (eV) | 23.84 | |
| $a$ (eV) | −0.58 | |
| $c$ (eV) | −0.58 | |

TABLE II. Comparison of band-gap and perturbation parameters; As $s$-orbital in GaAs.

| Channel | $j=81$ | $j=43$ |
|---|---|---|
| $2\delta a_i$ (eV) | 1.40 | 2.42 |
| $4\delta b_i$ (eV) | 1.38 | 2.37 |
| $\Delta E_i$ (eV) | 1.55 | 2.47 |
| $a\pm 2b\cos(\theta_i/2)$ (eV) | 0.63 | −8.67 |
| $g_i$ (eV) | 0.77 | −8.73 |
| $\omega_i/\pi$ | 0.50 | 0.77 |
| $(\gamma_i+\theta_i/2)/\pi$ | 0.49 | 0.77 |
| $4b$ (eV) | 24.40 | |
| $B$ (eV) | 24.60 | |
| $a$ (eV) | −0.17 | |
| $c$ (eV) | −0.25 | |

transforms. Very small features, such as the small peak at channel 63 in Fig. 6, are different in the various cases. Comparison of the perturbation results for the different orbitals gives results similar to those shown in the tables. The results for the size of the small conduction to conduction-band gap in Si is a little better for the $s^*$ and $p$ orbitals than for the $s$ orbitals shown in Table I.

Several approaches to construct a projected density of states from a finite set of recursion coefficients have been suggested.[3–6] Here we use a very simple termination scheme. The termination function in Eq. (5) is taken to have the form of the continued fraction for constant recursion coefficients $a$ and $b$,

$$t(E)=\frac{(E-a)-[(E-a)^2-4b^2]^{1/2}}{2b^2}\ . \tag{19}$$

The values of $a$ and $b$ are determined by the Fourier analysis. The calculated recursion coefficients do not approach a constant asymptotically. We linearly interpolate between the calculated coefficients $a_n$ and the constant value $a$ implied by Eq. (19),

$$\tilde{a}_n=\begin{cases} a_n, & n<n_1 \qquad (20a)\\ \dfrac{a_n(n_2-n)+a(n-n_1)}{n_2-n_1}, & n_1\le n\le n_2, \qquad (20b)\end{cases}$$

where $\tilde{a}_n$ is the value of the recursion coefficient used in the projected density-of-states calculation. The recursion coefficients $\tilde{b}_n$ used in the projected density-of-states calculation are found in an analogous way. Here, $n_1$ is the start of the interpolation and $n_2$ is the end. Recursion coefficients with $n>n_2$ are taken as constants and are included by the use of the terminating function. The values $n_1=50$ and $n_2=140$ were used.[20] From this set of recursion coefficients and this terminating function the projected densities of states are calculated using standard methods.[4]

In Figs. 8 and 9, we compare projected densities of states calculated using the recursion method and the termination scheme described above with those calculated

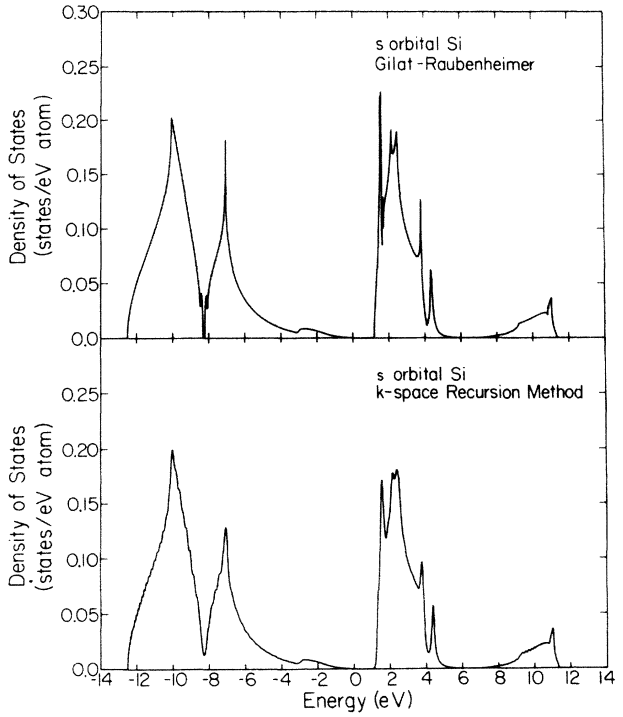


FIG. 8. $s$ orbital projected density of states in Si calculated with the recursion method (lower panel) and by Gilat-Raubenheimer integration (upper panel).

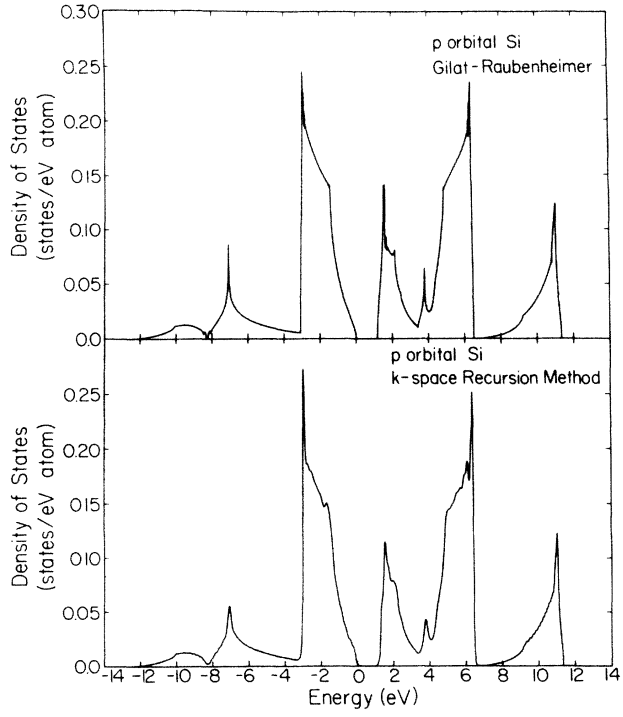


FIG. 9. $p$ orbital projected density of states in Si calculated with the recursion method (lower panel) and by Gilat-Raubenheimer integration (upper panel).

using Gilat-Raubenheimer integration[11] for the $s$ and $p$ orbitals of Si, respectively. Even using this simple terminating scheme, which can surely be improved upon, the recursion calculation yields a rather good density of states.

## IV. SUMMARY AND CONCLUSION

We have shown that by using a unitary transformation to $\mathbf{k}$ space and the special-$\mathbf{k}$-point method for evaluating Brillouin-zone sums, the recursion method can be very effectively applied to translationally invariant systems. We have used this approach to perform recursion calculations for tight-binding Hamiltonians of diamond- and zinc-blende-structure semiconductors.[10] For these Hamiltonians, we calculate 63 exact levels of recursion. The asymptotic behavior of the recursion coefficients was studied by Fourier analysis. The band gaps in the projected density of states dominate the asymptotic behavior. Perturbation results[16,17] describe the asymptotic behavior rather well. Projected densities of states were calculated using a very simple termination scheme. These densities of states compare favorably with the results of Gilat-Raubenheimer integration.

## ACKNOWLEDGMENTS

We have benefited from the use of the Cambridge Recursion Library, provided by the Theory of Condensed Matter group at Cambridge, and also advice and computer programs for Gilat-Raubenheimer integration provided by R. J. Hauenstein. One of us (S.M.A.) wishes to acknowledge hospitality and support from Los Alamos National Laboratory (Groups P-8 and E-11). The work of S.M.A. was supported by Eastman Kodak Company and by the U.S. Department of Energy, Project Agreement No. DE-AT03-81ER10870 under Contract No. DE-AM03-76SF00767. The work of D.L.S. was supported by Los Alamos National Laboratory Internal Supporting Research.

## APPENDIX: CONSTRUCTION OF THE SYMMETRIC k-SPACE FUNCTIONS

In this appendix, we describe how symmetry can be used to construct the symmetric functions defined in Eq. (12) where $g(\mathbf{k})$ is either the function summed in Eq. (10b) or in Eq. (10c). We use spatial symmetry and time-reversal symmetry. We first consider the case that the Hamiltonian commutes with time reversal and $U_0$ is a time-reversal eigenstate. In that case, one verifies that $U_n$ is a time-reversal eigenstate, for all $n$, with the same eigenvalue as $U_0$. One then finds that

$$g(\mathbf{k})=g(-\mathbf{k}) , \tag{A1}$$

for both of the $g$ functions.

The point group of operators $\{T_i\}$ (call it $G$) contains the inversion operator because it is the point group of a lattice. Let the group, $L$, contain the operators $\{l_i\}$ and have the property that

$$G=L\times C_i . \tag{A2}$$

Finally, let the group $Q$, containing the $n_s$ operators $\{S_i\}$, be the point group whose symmetry we will use. $Q$ must be a subgroup of the crystal- (lattice plus basis) point group. It should equal the crystal-point group if this group lacks the inversion operator and be a subgroup in which inversion is excluded if the crystal-point group contains inversion. The group $L$ is chosen [Eq. (A2) does not provide a unique definition] so that $Q$ is a subgroup of $L$. [These seemingly roundabout definitions are convenient because it allows one to use time reversal, rather than spatial inversion, to relate $g(\mathbf{k})$ and $g(-\mathbf{k})$. Restrictions on the state $U_0$ are thus reduced.]

Using Eq. (A1), we can reduce the expression for $f(\mathbf{k})$ to

$$f(\mathbf{k})=\frac{1}{n_l}\sum_i g(l_i\mathbf{k}) , \tag{A3}$$

where $n_l=n_T/2$ is the number of elements in $L$. If $Q$ is a proper subgroup of $L$, we define the set of $k$ points

$$\{l_i\mathbf{k}\}=\{S_j\mathbf{k},(S_j\mathscr{L}_1)\mathbf{k},\cdots\} , \tag{A4}$$

where $\mathscr{L}_1$, etc., are specific elements of $L$. This separation is just a resolution of $L$ in right cosets with respect to $Q$. Unless symmetry has deliberately been neglected in the choice of $Q$, there will be at most two elements $\mathscr{L}_1$ (the identity and one other). The expression for $f(\mathbf{k})$ may be written as

$$f(\mathbf{k})=\frac{n_s}{n_l}\sum_i\left[\frac{1}{n_s}\sum_j g[S_j(\mathscr{L}_i\mathbf{k})]\right] . \tag{A5}$$

The sum on $i$ must be done without help from symmetry, the sum on $j$ can be reduced using spatial symmetry.

Starting with the state function $U_0$, we construct the set $\{U_0^j\}$ where,

$$U_0^j\equiv S_jU_0 . \tag{A6}$$

One verifies that if $U_0^j$ is started through the recursion scheme, the same set of recursion coefficients $\{a_n,b_n\}$ are found as when $U_0$ is started through. The state functions $U_n^j$ generated in this way are related to those generated by starting with $U_0$ by

$$U_n^j=S_jU_n . \tag{A7}$$

If the set of functions $\{U_0^j\}$ is linearly dependent, the sum in Eq. (A5) can be simplified using symmetry. In this case, we can write

$$U_0^j=\sum_J\alpha_{jJ}U_0^J \tag{A8}$$

where $\{U_0^J\}$ is a linearly independent subset of $\{U_0^j\}$. One verifies that

$$U_n^j=\sum_J\alpha_{jJ}U_n^J . \tag{A9}$$

One also shows that for both of the $g$ functions considered

$$g^j(S_j\mathbf{k})=g(\mathbf{k}) , \tag{A10}$$

where $g^j(\mathbf{k})$ is the function calculated starting with $U_0^j$. Therefore,

$$\sum_j g(S_j\mathbf{k})=\sum_j g^j(\mathbf{k}) . \tag{A11}$$

Using Eq. (A9), we have

$$\sum_j \left[\sum_b \tilde{U}^*_{nb}(S_j\mathbf{k})\tilde{U}_{nb}(S_j\mathbf{k})\right] = \sum_j \sum_{J,J'} (\alpha_{jJ})^*\alpha_{jJ'} \left[\sum_b \tilde{U}^{*J}_{nb}(\mathbf{k})\tilde{U}^{J'}_{nb}(\mathbf{k})\right] \tag{A12}$$

and an analogous equation for the other $g$ function.

The set $\{U_0^J\}$ forms basis functions for a representation of the group $Q$,

$$S_j U_0^J=\sum_{J'} U_0^{J'} D_{J'J}(j) . \tag{A13}$$

The representation matrices are related to the expansion coefficients $\alpha_{jJ}$ by

$$D_{J'J}(j)=\alpha_{iJ'} , \tag{A14a}$$

where

$$S_i=S_jS_J . \tag{A14b}$$

Therefore, we can write

$$\sum_j (\alpha_{j,j})^*\alpha_{j,J'}=\sum_j D^*_{J,J''}(j)D_{J',J''}(j) , \tag{A15}$$

for any $J''$. If the representation is irreducible and unitary,

$$\sum_j D^*_{J,J''}(j)D_{J',J''}(j)=\frac{n_s}{n_J}\delta_{J,J'} , \tag{A16}$$

where $n_J$ is the dimension of the irreducible representation. In this case we have

$$\frac{1}{n_s}\sum_j g(S_j\mathbf{k})=\frac{1}{n_J}\sum_J g^J(\mathbf{k}) . \tag{A17}$$

This is our main result. The calculation can be greatly simplified if $U_0$ transforms according to a column of an irreducible representation. This is the usual case of interest because the Green's operator $(E-H)^{-1}$ does not mix functions which transform according to different irreducible representations or different columns of the same irreducible representation. Thus, in general, one can just break $U_0$ into pieces which transform according to the various irreducible representations. Equivalently, one can reduce the representation in Eq. (A13) if it is not irreducible.


[1]R. Haydock, in *Solid State Physics,* edited by H. Ehrenreich, F. Seitz, and D. Turnbull (Academic, New York, 1980), Vol. 35, p. 215.

[2]R. Haydock, in *The Recursion Method and its Applications,* edited by D. G. Pettifor and D. L. Wearie (Springer-Verlag, Berlin, 1985), p. 8.

[3]C. M. M. Nex, J. Phys. A **11**, 653 (1978).

[4]C. M. M. Nex, Comp. Phys. Commun. **34**, 101 (1984).

[5]R. Haydock and C. M. M. Nex, J. Phys. C **17**, 4783 (1984).

[6]G. Allan, J. Phys. C **17**, 3945 (1984).

[7]A. Baldereschi, Phys. Rev. B **7**, 5212 (1973).

[8]D. J. Chadi and M. L. Cohen, Phys. Rev. B **8**, 5747 (1973).

[9]H. J. Monkhorst and J. D. Pack, Phys. Rev. B **13**, 5188 (1976).

[10]P. Vogl, H. P. Hjalmarson, and J. D. Dow, J. Phys. Chem. Solids **44**, 365 (1983).

[11]G. Gilat and L. J. Raubenheimer, Phys. Rev. **144**, 390 (1966).

[12]The results can be generalized to a nonorthonormal basis. See, for example, Ref. 1.

[13]U. Brustel and K. Unger, Phys. Status Solidi B **123**, 229 (1984).

[14]For both diamond and zinc-blende structure materials $O_h$ is the group of operators $\{T_i\}$ called $G$ in the Appendix. For the diamond structure, $O_h$ is the crystal-point group and for the zinc-blende structure, $T_d$ is the crystal-point group. For both cases we take the groups $L$ and $Q$, defined in the Appendix, to be $T_d$.

[15]C. H. Hodges, J. Phys. (Paris) Lett. **38**, L187 (1977).

[16]D. M. Bylander and J. J. Rehr, J. Phys. C **13**, 4157 (1980).

[17]P. Turchi, F. Ducastelle, and G. Treglia, J. Phys. C **15**, 2891 (1982).

[18]We have slightly modified the tight-binding parameters of Ref. 10, to close a small, spurious, gap that would otherwise appear for $\alpha$-Sn.

[19]The coefficients $A_j$ and $B_j$ are point-wise defined. A continuous curve is shown for ease of view.

[20]The results of the density-of-states calculations are weakly dependent on the choice of $n_1$ and $n_2$.